

# Journal of Materials Chemistry B

Accepted Manuscript



This is an *Accepted Manuscript*, which has been through the Royal Society of Chemistry peer review process and has been accepted for publication.

*Accepted Manuscripts* are published online shortly after acceptance, before technical editing, formatting and proof reading. Using this free service, authors can make their results available to the community, in citable form, before we publish the edited article. We will replace this *Accepted Manuscript* with the edited and formatted *Advance Article* as soon as it is available.

You can find more information about *Accepted Manuscripts* in the [Information for Authors](#).

Please note that technical editing may introduce minor changes to the text and/or graphics, which may alter content. The journal's standard [Terms & Conditions](#) and the [Ethical guidelines](#) still apply. In no event shall the Royal Society of Chemistry be held responsible for any errors or omissions in this *Accepted Manuscript* or any consequences arising from the use of any information it contains.

**An electrochemiluminescence biosensor for sensitive and selective detection of Hg<sup>2+</sup> based on  $\pi$ - $\pi$  interaction between nucleotide and ferrocene-graphene nanosheets**

Bangrong Zhuo,<sup>†a</sup> Yuqin Li,<sup>†b</sup> An Zhang,<sup>a</sup> Fushen Lu,<sup>a</sup> Yaowen Chen<sup>c</sup> and Wenhua Gao<sup>\*ac</sup>

<sup>a</sup> Department of Chemistry, Shantou University, Shantou, Guangdong 515063, P. R. China. E-mail: [whgao@stu.edu.cn](mailto:whgao@stu.edu.cn); Fax: +86-22-82903941; Tel: +86-22-86502774

<sup>b</sup> Department of Pharmacy, Taishan Medicine College, Taian, Shandong 271016, P. R. China.

<sup>c</sup> Analysis & Testing Center, Shantou University, Shantou, Guangdong 515063, P. R. China.

<sup>†</sup> Bangrong Zhuo and Yuqin Li contributed equally to this work.

## Abstract

A solid-state electrochemiluminescence (ECL) biosensor based on DNA-modified electrode platform that depends on the variation of  $\pi$ - $\pi$  interaction before and after the binding of target analytes is put forward. The single-stranded DNA (ssDNA) probe was successfully assembled on the surface of glassy carbon electrode (GCE) which was pre-modified with  $\text{Ru}(\text{bpy})_3^{2+}$  complex and gold nanoparticles (GNPs). The ssDNA probe could strongly adsorb graphene due to the stronger  $\pi$ - $\pi$  interaction between nucleotide and graphene (GN), while in the presence of  $\text{Hg}^{2+}$ , the conformational transformation of DNA from single-stranded to double-stranded could result in an inhibited adsorption of GN. With thymine (T)-rich ssDNA as  $\text{Hg}^{2+}$  prober, we prepared the ECL biosensor by using ferrocene-graphene (Fc-GNs) as quenching unit to quench the ECL emission of  $\text{Ru}(\text{bpy})_3^{2+}$ , and the  $\text{Hg}^{2+}$  can be detected by the quenching efficiency transformation when the Fc-GNs getting away from  $\text{Ru}(\text{bpy})_3^{2+}$ . The biosensor exhibited sensitive response to various ranges of concentration of  $\text{Hg}^{2+}$  with a detection limit of 18 pM. The ECL biosensor held a great promise in the highly sensitive and selective detection of  $\text{Hg}^{2+}$  in natural water.

## 1. Introduction

Mercuric ion ( $\text{Hg}^{2+}$ ) is a major environmental pollutant and it is estimated by the United Nations Environment Programme (UNEP) that *ca.* 7500 tons of mercury is released into the environment annually. Mercuric ion, is known for its high toxicity and can cause many toxic effects to human body. It affects the immune system, alters genetic and enzyme systems, damages the nervous system, and can result in several diseases including acrodynia, kidney failure as well as minamata disease.<sup>1-3</sup> To date, several kinds of technologies have been developed for detecting  $\text{Hg}^{2+}$  ions, such as atomic absorption spectroscopy, cold vapor atomic fluorescence spectrometry and gas chromatography, etc.<sup>4</sup> Although these techniques are quite highly sensitive, selective and accurate for  $\text{Hg}^{2+}$  assay, many of these methods require complicated and multistep sample preparation or sophisticated instrumentations. Above all, these methods couldn't meet the requirement of quick detection of  $\text{Hg}^{2+}$ . It is reported that  $\text{Hg}^{2+}$  could specifically bind two DNA thymine (T) bases and promote the T-T mismatch forming stable base pairs.<sup>5,6</sup> According to this principle, biosensors based on electrochemiluminescence (ECL) for detection of  $\text{Hg}^{2+}$  have been developed due to their simple instrumentation and rapid response to the target substances.

Electrochemiluminescence is a well-known detection method that provides high sensitivity and selectivity through the generation of an optical signal triggered by an electrochemical reaction.<sup>7</sup> As kind of most widely presented ECL reagent, tris(2,2'-bipyridine)ruthenium(II) [ $\text{Ru}(\text{bpy})_3^{2+}$ ] has attracted much attention during the

past several decades due to its unique advantages of good electrochemical stability, high ECL efficiency and the convenience to couple with various measurement techniques.<sup>8,9</sup> However, the continuous consumption of  $\text{Ru}(\text{bpy})_3^{2+}$  in solution limits the widespread application of  $\text{Ru}(\text{bpy})_3^{2+}$  ECL sensors.<sup>10</sup> Since  $\text{Ru}(\text{bpy})_3^{2+}$  can be regenerated during the ECL reaction, it's possible and necessary to find a convenient method to realize the  $\text{Ru}(\text{bpy})_3^{2+}$  immobilization on the electrode surface to reduce the consumption of expensive ECL reagent and simplify experimental design.<sup>11,12</sup> Up to now, many methods have been reported about the immobilization of  $\text{Ru}(\text{bpy})_3^{2+}$  on the electrode surface. For example,  $\text{Ru}(\text{bpy})_3^{2+}$  has been incorporated with Langmuir-Blodgett films,<sup>13</sup> polymer films<sup>14</sup> and sol-gel composites.<sup>15</sup> Besides, our previous work have developed a novel approach to immobilize the  $\text{Ru}(\text{bpy})_3^{2+}$  by graphene film *via* in situ wet-chemical reduction of graphene oxide (GO).<sup>16</sup> Nevertheless, these methods with the requirement of additional substances are complicated to the experimental design. In another work, Soo Beng Khoo *et al.*<sup>17</sup> reported that  $\text{Ru}(\text{bpy})_3^{2+}$  complex molecules were directly attached to the solid glassy carbon surface of glassy carbon electrode (GCE) without using any additional host matrices. Herein, we immobilized the  $\text{Ru}(\text{bpy})_3^{2+}$  on the GCE by a brief potentiostatic approach which applying a high anodic potential on the bare GCE in the  $\text{Ru}(\text{bpy})_3^{2+}/\text{KNO}_3$  solution. A rimous structure was formed on the glassy carbon surface of the GCE and the co-deposition of the glassy carbon with the  $\text{Ru}(\text{bpy})_3^{2+}$  complex led to the stable immobilization of the  $\text{Ru}(\text{bpy})_3^{2+}$  complex.

Graphene (GN), as a one-atom-thick sheet of  $\text{sp}^2$ -bonded carbon atoms in a closely

packed honeycomb lattice, with unique electrical conductivity, extraordinary surface area,<sup>18</sup> high potential for mass production and easy functionalization,<sup>19</sup> has revealed enormously promising gateways for rapid progress in various scientific and technological fields, such as biophysics and biotechnology.<sup>20-23</sup> Particularly, by virtue of the high surface area, high  $\pi$ -conjugation and hydrophobic properties, GN can provide a platform for immobilizing organic and inorganic molecules, which promote the development of graphene-based sensors.<sup>24, 25</sup> GN could be strongly adsorbed on the ssDNA probe due to the strong  $\pi$ - $\pi$  stacking between nucleotide and GN, and inhibit the desorption of GN when the probe bound the specific target to form a double helix. The study on the unique interactions of GN and nucleotide has been well developed in the electrochemical biosensing. Shaojun Dong *et al.*<sup>26</sup> designed an excellent electrochemical aptasensor by taking the advantage of the ultrahigh electron transfer ability of GN and its unique GN/ssDNA interaction. However, the mechanism of the distinctive GN/ssDNA interaction has not been well employed to fabricate ECL biosensors. Thus, we designed a brief ultra-sensitive ECL biosensor preparation method by utilizing the ssDNA to adsorb the ferrocene-graphene nanosheets (Fc-GNs), and take the Fc-GNs as quenching unit to quench the ECL emission of  $\text{Ru}(\text{bpy})_3^{2+}$ .

In the present work, thiolated-ssDNA probe was successfully anchored on the gold nanoparticles (GNPs) through the thiol-Au bond to assemble the monolayer of ssDNA on the surface of GCE. A thiolated 28-mer T-rich ssDNA was designed to capture  $\text{Hg}^{2+}$  in the light of the theory that  $\text{Hg}^{2+}$  could specifically bind two DNA thymine (T) bases and promote the T-T mismatch to form stable base pair. As shown in Scheme 1, firstly,

the GCE modified by  $\text{Ru}(\text{bpy})_3^{2+}$  complex molecules and GNPs formed a platform for the self-assembly of T-rich ssDNA. Secondly, the biosensing electrode was immersed into a certain concentration of Fc-GNs solution. Due to the strong  $\pi$ - $\pi$  interaction, the Fc-GNs was adsorbed on the ssDNA and effectively quenched the ECL intensity of  $\text{Ru}(\text{bpy})_3^{2+}$  complex. Finally, in presence of  $\text{Hg}^{2+}$ , the T-rich ssDNA binding  $\text{Hg}^{2+}$  to form T- $\text{Hg}^{2+}$ -T stable base pairs and get the conformational transition of ssDNA to C-type dsDNA, coincided with the transformation of luminescence signal from “off” to “on”. By employing this strategy, the ECL biosensor was successfully applied in ultrasensitive detection of  $\text{Hg}^{2+}$  in natural water.

[Scheme 1]

## 2. Experimental

### 2.1 Reagents and Apparatus

Oligonucleotide was purchased from Sangon Bioengineering Ltd. Company (Shanghai, China) and the sequence is shown as follows:



Tris (2, 2'-bipyridyl) ruthenium (II) chloride hexahydrate, 2-mercaptohexanol (MCH), mercury nitrate ( $\text{Hg(NO}_3\text{)}_2$ ) and other metal salts were purchased from Sigma-Aldrich (St. Louis, MO, USA). Tri-*n*-propylamine (TPrA), ferrocene-carboxaldehyde (FcCHO) and Tetrachloroauric (III) acid tetrahydrate ( $\text{HAuCl}_4 \cdot 4\text{H}_2\text{O}$ ) were obtained from Aladdin Chemical Reagent Co. Ltd. (Shanghai, China). Sodium borohydride ( $\text{NaBH}_4$ ) was obtained from Beijing Chemical Factory (Beijing, China). Ethylenediamine (ED) and N, N'-Dicyclohexyl-carbodiimide (DCC, 99%) were purchased from Sinopharm Chemical Reagent Co. Ltd. (Shanghai, China). All other chemicals not mentioned here were of analytical reagent grade and were used as received. Millipore Milli-Q water ( $18 \text{ } \Omega\text{M cm}$ ) supplied by a Millipore Milli-Q water purification system (Bedford, MA, USA) was used throughout the process. The working solutions were prepared by diluting stock solution with phosphate buffer solution (PBS, pH 7.50, 0.10 M NaCl + 0.10 M  $\text{NaH}_2\text{PO}_4/\text{Na}_2\text{HPO}_4$ ) and deionized water. All measurements were carried out at room temperature,  $24 \pm 2^\circ\text{C}$ .

A traditional three-electrode system composed of a bare GCE (3 mm in diameter) or

biosensor as working electrode, a platinum wire as counter electrode and a Ag/AgCl (1 M KCl) as reference electrode was applied in a 10 mL glassy analytical cell. Cyclic voltammetry (CV) curves and electrochemical impedance spectroscopy (EIS) were measured with IM6ex electrochemical workstation (Zahner IM6ex, Germany). ECL detections were carried out with a MPI-B ECL Analyzer Systems (Remax, China). Fourier Transform-Infrared (FT-IR) spectra were recorded on a Magna 750 FTIR spectrophotometer (Nicolet, USA) as KBr pellets. The scanning electron microscope (SEM, JSM-6360LA, JEOL, Japan) was used to observe the modified electrodes. Atomic force microscopy (AFM) was performed on a Digital Instruments Nanoscope IIIa (Veeco, CA). The electron micrographs of GO and Fc-GNs were taken by using a transmission electron microscope (TEM, JEM-1400, JEOL, Japan). A PHS-3CA precision pH meter (Dapu, China) was used in the experiment. Sample analysis was performed with Atomic Fluorescence Spectrometer (AFS-230E, China).

## **2.2 Electrode cleaning, conditioning and electrochemical deposition of Ru(bpy)<sub>3</sub><sup>2+</sup> and GNPs**

GCEs with the glassy carbon (GC) rod diameter of 3 mm were polished with 0.3 μm and 0.05 μm alumina slurry (Al<sub>2</sub>O<sub>3</sub>) on polishing cloth sequentially. The electrodes were fully rinsed after each polishing step and finally sonicated in deionized water and anhydrous ethanol for 5 min respectively, followed by electrochemical conditioning by potential scanning from -0.2 V to 1.6 V in 0.5 M H<sub>2</sub>SO<sub>4</sub> for at least five complete scans at 100 mV·s<sup>-1</sup> until the reproducible cyclic voltammogram was obtained. Then

the electrode was immediately used for deposition modification after a rinse step.

The immobilization of  $\text{Ru}(\text{bpy})_3^{2+}$  was based on the modified electrochemical method.<sup>17</sup> The  $\text{Ru}(\text{bpy})_3^{2+}$  complex molecules were electrodeposited on the glassy carbon surface of GCE by applying a high anodic potential of 1.8 V for 300 s in 0.1 mM  $\text{Ru}(\text{bpy})_3^{2+}$  complex, 0.01 M potassium nitrate ( $\text{KNO}_3$ ) solution. After a rinse step with deionized water, the GCE/ $\text{Ru}(\text{bpy})_3^{2+}$  electrode was immersed into 100  $\mu\text{M}$  of  $\text{HAuCl}_4$  solution in 5 mL of 0.5 M  $\text{KNO}_3$  and applying a 5 s potential step from 1.1 to -1.0 V to deposit the GNPs according to our previous experimental work.<sup>27</sup>

### 2.3 Preparation of Fc-GNs

GO was prepared from graphite flake based on the modified Hummers method.<sup>28</sup> Fc-GNs were synthesized according to the previously reported method.<sup>29</sup> The Fc-GNs was characterized by FT-IR spectroscopy (Fig. S1), AFM and TEM images (Fig. S2) so as to verify that ferrocene (Fc) was indeed grafted onto the surface of graphene nanosheets. More details of the Fc-GNs synthesis can be found in the supporting information.

### 2.4 Fabrication of biosensing electrode

The electrode modified by electrodeposited  $\text{Ru}(\text{bpy})_3^{2+}$  complex molecules and GNPs was first immersed into the 10  $\mu\text{M}$  DNA solution in order to assemble the monolayer of ssDNA probe through the thiol-Au bond between thiolated-DNA probe and GNPs. The distribution and orientation of ssDNA was well controlled by the GNPs rather than simply sprawling the ssDNA strands on the planar gold electrode

according to our previous experimental work.<sup>27</sup> The assembly process was kept for at least 3 h at room temperature, followed by being thoroughly washed in a stirred solution of PBS solution for 20 min to remove any weakly bound DNA strands. In order to obtain well-aligned DNA monolayer with the probe strands nearly perpendicular to the surface of electrode, the electrode was finally treated with 1 mM MCH solution for 1 h at room temperature and washed again in the stirred solution of PBS solution for 20 min. Then the electrode was immersed into the 2.0 mg·mL<sup>-1</sup> Fc-GNs solution for at least 1 h. Finally, the modified electrode was carefully washed to remove the unfixed Fc-GNs aggregations with deionized water, and then the ECL biosensor was obtained.

### 2.5 ECL measurement of Hg<sup>2+</sup>

Various ranges of concentration of Hg<sup>2+</sup> were prepared for determining the sensitivity of this ECL biosensor by serial dilution of the Hg(NO<sub>3</sub>)<sub>2</sub> stock solution. After a pre-scan to record the luminescence intensity of the “signal-off” sensor, the sensor was immersed into 100 μL PBS solution containing certain concentration of Hg<sup>2+</sup> for 30 min at room temperature followed by washing for at least 5 min with 0.1 M PBS solution and deionized water to remove any unbound substances.

The ECL determinations were performed at room temperature and CV mode with continuous potential scanning from 0.2 V to 1.25 V at a scanning rate of 100 mV·s<sup>-1</sup> was applied to achieve ECL signals in 0.1 M PBS (pH 7.50, 0.10 M NaCl + 0.10 M NaH<sub>2</sub>PO<sub>4</sub>/Na<sub>2</sub>HPO<sub>4</sub>) containing 0.1 M TPrA. The supersaturated TPrA solution was

prepared as previous protocol.<sup>30</sup> A negative high voltage of -800 V was supplied to the photomultiplier for luminescence intensity determination.

### 3. Results and discussion

#### 3.1 Characterization of the electrode electrodeposited $\text{Ru}(\text{bpy})_3^{2+}$ and GNPs

In order to obtain the information on the change of the GCE and after electrodeposited the  $\text{Ru}(\text{bpy})_3^{2+}$  complex molecules and GNPs, Cyclic Voltammetry (CV) curves were carried out. The bare GCE and the modified GCE were used for CV measurement. As shown in Fig. 1A, curve a exhibited the bare GCE in 0.05 M  $\text{H}_2\text{SO}_4$  solution at the scan rate of  $100 \text{ mV}\cdot\text{s}^{-1}$  and the curve was smooth without obvious reversible peak. Following the electrodeposited of the GNPs on the surface of the GCE, curve b exhibited a reduction potential at 0.68 V and indicated that the GNPs modified GCE was obtained. As shown in Fig. 1B, after applying a high anodic potential of 1.8 V on the bare GCE for 300 s in  $\text{Ru}(\text{bpy})_3^{2+}/\text{KNO}_3$  solution, a reversible peak ( $E^0=1.03 \text{ V}$ ) was observed (curve a), indicated that the  $\text{Ru}(\text{bpy})_3^{2+}$  complex molecules were immobilized on the glassy carbon surface of GCE. Curve b showed the  $\text{Ru}(\text{bpy})_3^{2+}$  and GNPs modified GCE ( $\text{GCE}/\text{Ru}(\text{bpy})_3^{2+}/\text{GNPs}$ ) in 0.05 M  $\text{H}_2\text{SO}_4$  solution at the scan rate of  $100 \text{ mV}\cdot\text{s}^{-1}$ . Another oxidation current peak at 1.23 V and reduction potential at 0.52 V was also observed in the curve d, this was probably due to the fact that the electrodeposited of GNPs affected the feature of the  $\text{GCE}/\text{Ru}(\text{bpy})_3^{2+}$  electrode. Continuous cycles of the  $\text{GCE}/\text{Ru}(\text{bpy})_3^{2+}/\text{GNPs}$  electrode showed excellent stability, confirming that the  $\text{Ru}(\text{bpy})_3^{2+}$  complex molecules were strongly bound on the glassy carbon surface of GCE. Furthermore, the conclusion was also supported by the SEM images of the modified GCE. It could be found that the

surface of the bare GCE (Fig. 2A) was smooth, while the GCE showed rimous surface topography after applying a high anodic potential of 1.8 V (Fig. 2B). It can be interpreted as that  $\text{Ru}(\text{bpy})_3^{2+}$  could be electrodeposited with the pre-modified GCE and make a stable  $\text{Ru}(\text{bpy})_3^{2+}$  modification effect. As shown in Fig. 2C, the size of the GNPs was uniform, and well-distributed on the surface of GCE. After electrodeposited the  $\text{Ru}(\text{bpy})_3^{2+}$  complex and GNPs on the surface of GCE, the SEM image (Fig. 2D) of the GCE/ $\text{Ru}(\text{bpy})_3^{2+}$ /GNPs electrode showed the  $\text{Ru}(\text{bpy})_3^{2+}$  complex and GNPs were steadily and uniformly immobilized on the surface of GCE.

[Fig. 1]

[Fig. 2]

### 3.2 Characterization of the biosensing electrode impedance

Electrochemical impedance spectroscopy (EIS) was adopted to monitor the fabrication processes of the biosensing electrode and characterize the impedance feature of nanopatterned GCE with  $\text{Ru}(\text{bpy})_3^{2+}$  complex molecules and GNPs. In the form of Nyquist plot, Fig. 3 shows the impedance spectra obtained in the investigation. The bare GCE gave an almost linear arc plot with a micro radian in high frequency region and behaved as an ideal conductor (curve a), indicating a very fast electron transfer process of  $[\text{Fe}(\text{CN})_6]^{3-/4-}$ . The immobilization of  $\text{Ru}(\text{bpy})_3^{2+}$ /GNPs on the GCE affected the impedance feature of the electrode and showed a large charge transfer resistance ( $R_{ct}$ ) than the bare GCE (curve b). After the self-assembly of the thiolated-DNA strands, owing to the strong  $\pi$ - $\pi$  interactions of ssDNA with Fc-GNs,

Fc-GNs could be preferentially adsorbed on the ssDNA and highly enhance the electron transfer process of  $[\text{Fe}(\text{CN})_6]^{3-/4-}$ . Therefore, a distinct decrease of electrochemical impedance can also be observed (curve c). The conformational transition of T-rich ssDNA induced by  $\text{Hg}^{2+}$  led to the desorption of Fc-GNs from double-stranded DNA (dsDNA) after the biosensing electrode incubated in certain concentration of  $\text{Hg}^{2+}$  for a period of time. It is obvious that the conformational transition could produce negative impedance performance and there is a slight increase in impedance (curve d).

[Fig. 3]

### 3.3 Optimum conditions

In order to obtain the optimal condition, several impact factors were optimized. We investigated the incubation time of ECL biosensor electrode with  $\text{Hg}^{2+}$ , the pH of the test solution and the salt concentration of the PBS solution.

#### 3.3.1 Incubation time

The effect of the incubation time on the performance of the biosensing electrode at  $\text{Hg}^{2+}$  concentration of 0.05, 1 and 100 nM was shown in Fig. 4. As the incubation time increased, the ECL intensity change ( $\Delta I_{\text{ECL}}$ ) increased rapidly and reached a plateau after 30 min suggesting that the T- $\text{Hg}^{2+}$ -T stands was forming gradually and an almost complete binding reached. Therefore, 30 min was chosen for further experiments.

[Fig. 4]

### 3.3.2 pH and the concentration of NaCl

To investigate the effect of pH on the ECL intensity, the test solution at diverse pH values (5.5 to 9.0 in intervals of 0.5, PBS: 0.10 M NaCl + NaH<sub>2</sub>PO<sub>4</sub>/Na<sub>2</sub>HPO<sub>4</sub>) were investigated. The ECL curves were measured in PBS containing 0.1 M TPrA after the Fc-GNs modified GCE biosensor immersed into 100 nM Hg<sup>2+</sup> solution. As shown in Fig. 5A, the best test solution was obtained at pH 7.50. This was probably due to the fact that the Hg<sup>2+</sup> exhibits weak coordination with DNA thymine (T) bases in acidic or alkaline solution.

The concentration of NaCl in the PBS solution was very important to the activity of DNA, while the activity of DNA could affect the performance of the biosensing electrode. Therefore, the concentration of NaCl played a dominant role in the detection. The ECL determinations of the biosensing electrode were performed in PBS (pH 7.50, 0.10 M NaH<sub>2</sub>PO<sub>4</sub>/Na<sub>2</sub>HPO<sub>4</sub> + NaCl) containing 0.1 M TPrA after the Fc-GNs modified GCE biosensor immersed into 100 nM Hg<sup>2+</sup> solution. As shown in Fig. 5B, the ECL intensity was enhanced as higher concentration of NaCl was added into the PBS solution, and reached a peak at the concentration was 0.1 M. Thus, 0.1 M was selected as the optimal concentration of NaCl for further experiments.

[Fig. 5]

### 3.4 Stability and reproducibility of the Hg<sup>2+</sup> biosensor

ECL method was used to prove that the monolayer of ssDNA probe was stably fabricated on the modified GCE in the 0.10 M PBS (pH 7.50, 0.10 M NaCl + 0.10 M NaH<sub>2</sub>PO<sub>4</sub>/Na<sub>2</sub>HPO<sub>4</sub>) containing 0.10 M TPrA using a linear potential scan technique.

To test the quencher function of  $\text{Ru}(\text{bpy})_3^{2+}$  complex and Fc-GNs, a 28-mer-DNA which is T-rich fragment was used to form a linear ssDNA and immobilized on the GNPs. Fc-GNs could be strongly adsorbed on the ssDNA due to strong  $\pi$ - $\pi$  interaction, resulting in effectively quenching the ECL intensity of  $\text{Ru}(\text{bpy})_3^{2+}$  complex. Fig. 6 shows that the  $\text{Ru}(\text{bpy})_3^{2+}$  complex electrodeposited on the GCE results in an obvious ECL signal response (curve b) in contrast with the bare GCE (curve a). After adsorbing the Fc-GNs, a striking decrease of ECL signal is found for the quenching effect of Fc to  $\text{Ru}(\text{bpy})_3^{2+}$  (curve c). The biosensor after incubation in certain concentration of  $\text{Hg}^{2+}$  could give an obvious enhanced ECL signal response (curve d). The result can be explained as that the  $\text{Hg}^{2+}$  induced the conformational transition of T-rich ssDNA and then the quenching effect of Fc to  $\text{Ru}(\text{bpy})_3^{2+}$  became weaker because of the desorption of Fc-GNs from dsDNA. Furthermore, as shown in the inset of Fig. 6, continuous CV scanning the electrodes can give a balanced ECL intensity, indicating that the biosensor has acceptable reliability and stability, the  $\text{Ru}(\text{bpy})_3^{2+}$  complex molecules were anchored on the GCE in form of  $\text{GCE}/\text{Ru}(\text{bpy})_3^{2+}$  without  $\text{Ru}(\text{bpy})_3^{2+}$  complex molecules escaping from the glassy carbon surface of GCE. The reproducibility of the biosensor was evaluated by analysis of the same concentration of  $\text{Hg}^{2+}$  (10 nM) using five biosensors under the same conditions. All biosensors exhibited closely ECL responses and the relative standard deviation (RSD) of 3.5% was obtained, which indicated that the reproducibility of the proposed biosensor was acceptable.

[Fig. 6]

### 3.5 Sensitivity and selectivity of the Hg<sup>2+</sup> biosensor

Under the optimized test condition, the sensitivity of ECL biosensors was assessed by measuring the dependence of the increased  $\Delta I_{\text{ECL}}$  upon the concentration of Hg<sup>2+</sup>. As shown in Fig. 7, the ECL intensity was enhanced when higher concentration of Hg<sup>2+</sup> was used for binding the T-rich ssDNA; and the  $\Delta I_{\text{ECL}}$  was found to be logarithmically related to the concentration of Hg<sup>2+</sup> in a range from 0.05 nM to 100 nM (inset of Fig. 7). The regression equation was  $\Delta I_{\text{ECL}} = 371 \lg C_{\text{Hg}^{2+}} + 4226.6$  with a regression coefficient of 0.9968 and detection limit of 18 pM which is defined as the concentration corresponding to the mean blank value plus 3 standard deviations. This limit of detection (LOD) is 3 orders of magnitude lower than the Maximum Contaminant Level in drinking water set forth by the United States Environmental Protection Agency (USEPA) in the Clean Water Act of 2 ppb (10 nM). The performance of different Hg<sup>2+</sup> sensors<sup>31-35</sup> is summarized in Table 1, which demonstrates that the detection limit of 18 pM in our work is highly sensitive.

[Fig. 7]

[Table 1]

The selectivity of the biosensor was examined by incubating the biosensor in the aqueous solutions containing Hg<sup>2+</sup>, while the control experiments were performed using various metal ions like Cu<sup>2+</sup>, Zn<sup>2+</sup>, Ni<sup>2+</sup>, Cd<sup>2+</sup>, Mg<sup>2+</sup>, Fe<sup>2+</sup>, Ba<sup>2+</sup>, Pb<sup>2+</sup>, Cr<sup>3+</sup>, Co<sup>2+</sup>, Mn<sup>2+</sup>, Fe<sup>3+</sup>, Al<sup>3+</sup> and Ca<sup>2+</sup> at a concentration of 500 nM and Hg<sup>2+</sup> at 10 nM, respectively. As shown in Fig. 8, the biosensor showed significant ECL intensity in response to Hg<sup>2+</sup>, but hardly exhibited substantial responses to other metal ions,

suggesting that the biosensor possessed excellent selectively response to  $\text{Hg}^{2+}$  against other environmentally relevant metal ions. Besides, we had performed experiment with natural water samples, the determination of  $\text{Hg}^{2+}$  concentration was performed by the standard addition method. As shown in Table S1, we observed that the results obtained in natural water samples showed good recovery values (97.78-101.89%), which confirmed that the interferences in water samples could be almost neglected and this developed biosensor showed a good selectivity for  $\text{Hg}^{2+}$ .

[Fig. 8]

### 3.6 Direct detection of $\text{Hg}^{2+}$ in water samples

The applications of the biosensor were evaluated for determination of  $\text{Hg}^{2+}$  in natural water. The concentration of  $\text{Hg}^{2+}$  was determined by the biosensing method as well as AFS method. The water samples were collected in the Xinhua River and Niutianyang bay in Shantou, China. The samples collected were filtered through 0.2  $\mu\text{m}$  membranes to remove impurities and diluted with equal volume of PBS (pH 7.50, 0.10 M NaCl + 0.10 M  $\text{NaH}_2\text{PO}_4/\text{Na}_2\text{HPO}_4$ ) solution. The results were summarized in Table 2 and showed good agreement with those achieved by using standard AFS method.

[Table 2]

#### 4. Conclusions

In conclusion, a solid-state ECL biosensor for the highly sensitive and selective detection of  $\text{Hg}^{2+}$  in aqueous solution has been developed. Employment of  $\text{Ru}(\text{bpy})_3^{2+}$  complex as an ECL label and strongly bounded on the surface of highly oxidized GC electrodes by a brief potentiostatic approach, the biosensor showed excellent and stable ECL intensity. The quench pattern of Fc-GNs to  $\text{Ru}(\text{bpy})_3^{2+}$  *via*  $\pi$ - $\pi$  interaction between nucleotide and Fc-GNs simplifies experimental design and performs a stable quenching effect on  $\text{Ru}(\text{bpy})_3^{2+}$ . Moreover, the optimized distribution and orientation of ssDNA which was well controlled by the GNPs played a great important role in the sensitivity of the biosensor to  $\text{Hg}^{2+}$ . In our present work, the presented biosensor has a detection limit of 18 pM, which is much lower than the USEPA limit of  $\text{Hg}^{2+}$  in drinkable water (<10 nM). In addition, this design of the biosensor does not require costly equipment and sophisticated sample pretreatment. In summary, a cost-effective and rapid method presented by our work make it possible for on-site detection of  $\text{Hg}^{2+}$  in real environmental water samples.

## Acknowledgements

We acknowledge financial support of this work by Research Start-up Funding of Shantou University (No. NTF10002), the Natural Science Foundation of Guangdong Province (No. S2011010005208), the National Natural Science Foundation of China (No. 51272152/E0208) and the Guangdong High Education Fund of Science and Technology Innovation (No. 2013KJCX0078).

## References

- 1 Q. R. Wang, D. Kim, D. D. Dionysiou, G. A. Sorial and D. Timberlake, *Environ. Pollut.*, 2004, **131**, 323-336.
- 2 P. W. Davidson, G. J. Myers and B. Weiss, *Pediatrics*, 2004, **113**, 1023-1029.
- 3 Y. Q. Lai, Y. Y. Ma, L. P. Sun, J. Jia, J. Weng, N. Hu, W. Yang and Q. Q. Zhang, *Electrochim. Acta.*, 2011, **56**, 3153-3158.
- 4 V. L. Dressler, F. G. Antes, C. M. Moreira, D. Pozebon and F. A. Duarte, *Int. J. Mass Spectrom.*, 2011, **307**, 149-162.
- 5 Y. Miyake, H. Togashi, M. Tashiro, H. Yamaguchi, S. Oda, M. Kudo, Y. Tanaka, Y. Kondo, R. Sawa, T. Fujimoto, T. Machinami and A. Ono, *J. Am. Chem. Soc.*, 2006, **128**, 2172-2173.
- 6 Y. Tanaka, S. Oda, H. Yamaguchi, Y. Kondo, C. Kojima and A. Ono, *J. Am. Chem. Soc.*, 2007, **129**, 244-245.
- 7 X. Y. Wang, W. Yun, P. Dong, J. M. Zhou, P. G. He and Y. Z. Fang, *Langmuir.*, 2008, **24**, 2200-2205.
- 8 M. M. Richter, *Chem. Rev.*, 2004, **104**, 3003-3036.
- 9 W. Miao, *Chem. Rev.*, 2008, **108**, 2506-2553.
- 10 H. Dai, Y. M. Wang, X. P. Wu, L. Zhang and G. N. Chen, *Biosens. Bioelectron.*, 2009, **24**, 1230-1234.
- 11 Z. H. Guo, Y. Shen, M. K. Wang, F. Zhao and S. J. Dong, *Anal. Chem.*, 2004, **76**, 184-191.

- 12 X. P. Sun, Y. Du, L. X. Zhang, S. J. Dong and E. K. Wang, *Anal. Chem.*, 2007, **79**, 2588-2592.
- 13 X. Zhang and A. J. Bard, *J. Phys. Chem.*, 1988, **92**, 5566-5569.
- 14 I. Rubinstein and A. J. Bard, *J. Am. Chem. Soc.*, 1981, **103**, 5007-5013.
- 15 M. M. Collinson, B. Novak, S. A. Martin and J. S. Taussig, *Anal. Chem.*, 2000, **72**, 2914-2918.
- 16 W. H. Gao, Y. S. Chen, J. Xi, A. Zhang, Y. W. Chen, F. S. Lu and Z. G. Chen, *Sensor: Actuat. B-Chem.*, 2012, **171-172**, 1159-1165.
- 17 J. Premkumar and S. B. Khoo, *Electrochem. Commun.*, 2004, **6**, 984-989.
- 18 D. Li, M. B. Muller, S. Gilje, R. B. Kaner and G. G. Wallace, *Nat. Nanotechnol.*, 2008, **3**, 101-105.
- 19 Y. Y. Shao, J. Wang, H. Wu, J. Liu, I. A. Aksay and Y. H. Lin, *Electroanal.*, 2010, **22**, 1027-1036.
- 20 H. Y. Mao, S. Laurent, W. Chen, O. Akhavan, M. Imani, A. A. Ashkaran and M. Mahmoudi, *Chem. Rev.*, 2013, **113**, 3407-3424.
- 21 K. Wang, Q. Liu, Q. M. Guan, J. Wu, H. N. Li and J. J. Yan, *Biosens. Bioelectron.*, 2011, **26**, 2252-2257.
- 22 D. B. Zhu, J. F. Liu, Y. B. Tang and D. Xing, *Sensor: Actuat. B-Chem.*, 2010, **149**, 221-225.
- 23 C. L. Sun, H. H. Lee, J. M. Yang and C. C. Wu, *Biosens. Bioelectron.*, 2011, **26**, 3450-3455.
- 24 Y. J. Li, W. Gao, L. J. Ci, C. M. Wang and P. M. Ajayan, *Carbon*, 2010, **48**,

- 1124-1130.
- 25 T. Kuila, S. Bose, P. Khanra, A. K. Mishra, N. H. Kim and J. H. Lee, *Biosens. Bioelectron.*, 2011, **26**, 4637-4648.
- 26 L. Wang, M. Xu, L. Han, M. Zhou, C. Z. Zhu and S. J. Dong, *Anal. Chem.*, 2012, **84**, 7301-7307.
- 27 W. H. Gao, A. Zhang, Y. S. Chen, Z. X. Chen, Y. W. Chen, F. S. Lu and Z. G. Chen, *Biosens. Bioelectron.*, 2013, **49**, 139-145.
- 28 W. S. Hummers and R. E. Offeman, *J. Am. Chem. Soc.*, 1958, **80**, 1339-1339.
- 29 L. S. Fan, Q. X. Zhang, K. K. Wang, F. H. Li and L. Niu, *J. Mater. Chem.*, 2012, **22**, 6165-6170.
- 30 S. J. Wang, M. T. Neshkova and W. J. Miao, *Electrochim. Acta.*, 2008, **53**, 7661-7667.
- 31 R. M. Kong, X. B. Zhang, L. L. Zhang, X. Y. Jin, S. Y. Huan, G. L. Shen and R. Q. Yu, *Chem. Commun.*, 2009, **37**, 5633-5635.
- 32 D. Han, Y. Kim, J. Oh, T. H. Kim, R. K. Mahajan, J. S. Kim, H. Kim, *Analyst*, 2009, **134**, 1857-1862.
- 33 S. J. Liu, H. G. Nie, J. H. Jiang, G. L. Shen, R. Q. Yu, *Anal. Chem.*, 2009, **81**, 5724-5730.
- 34 X. Zhu, L. F. Chen, Z. Y. Lin, B. Qiu and G. N. Chen, *Chem. Commun.*, 2010, **46**, 3149-3151.
- 35 C. X. Tang, Y. Zhao, X. W. He and X. B. Yin, *Chem. Commun.*, 2010, **46**, 9022-9024.

**Figure captions:**

**Scheme 1** Schematic illustration of the ECL biosensor for  $\text{Hg}^{2+}$  detection.

**Fig. 1** Continuous cyclic voltammograms of A: the bare GCE (a) and the GNPs modified GCE (b), B: the  $\text{GCE}/\text{Ru}(\text{bpy})_3^{2+}$  modified electrode (a) and the  $\text{GCE}/\text{Ru}(\text{bpy})_3^{2+}/\text{GNPs}$  modified electrode (b) in 0.05 M  $\text{H}_2\text{SO}_4$  solution at the scan rate of  $100 \text{ mV}\cdot\text{s}^{-1}$ .

**Fig. 2** SEM images of bare GC electrode surface (A),  $\text{GCE}/\text{Ru}(\text{bpy})_3^{2+}$  modified electrode (B), GNPs modified GCE (C) and the  $\text{GCE}/\text{Ru}(\text{bpy})_3^{2+}/\text{GNPs}$  modified electrode (D).

**Fig. 3** Nyquist plot for electrochemical impedance measurements in 5.0 mM  $[\text{Fe}(\text{CN})_6]^{3-/4-}$  solution for the bare GCE (a), the  $\text{GCE}/\text{Ru}(\text{bpy})_3^{2+}/\text{GNPs}$  electrode (b), the Fc-GNs modified GCE biosensor (c) and GCE biosensor after binding with  $\text{Hg}^{2+}$  (d).

**Fig. 4** Incubation time of ECL biosensing electrode with  $\text{Hg}^{2+}$  with concentration of 0.05 nM, 1 nM and 100 nM. ECL intensity was measured in 0.1 M PBS (pH 7.50, 0.10 M  $\text{NaCl}$  + 0.10 M  $\text{NaH}_2\text{PO}_4/\text{Na}_2\text{HPO}_4$ ) containing 0.1 M TPrA. Scan rate:  $100 \text{ mV}\cdot\text{s}^{-1}$ , scan range: 0.2-1.25 V.

**Fig. 5** The effect of pH (A) and NaCl concentration (B). A: ECL intensity was measured in PBS (0.10 M NaCl + NaH<sub>2</sub>PO<sub>4</sub>/Na<sub>2</sub>HPO<sub>4</sub>) containing 0.1 M TPrA. Scan rate: 100 mV·s<sup>-1</sup>, scan range: 0.2-1.25 V. B: ECL intensity was measured in PBS (NaCl + 0.10 M NaH<sub>2</sub>PO<sub>4</sub>/Na<sub>2</sub>HPO<sub>4</sub>) containing 0.1 M TPrA. Scan rate: 100 mV·s<sup>-1</sup>, scan range: 0.2-1.25 V.

**Fig. 6** ECL intensity vs potential curves for the bare GCE (a), the GCE/Ru(bpy)<sub>3</sub><sup>2+</sup>/GNPs electrode (b), the Fc-GNs modified GCE biosensor (c) and GCE biosensor after binding with Hg<sup>2+</sup> (d). Inset: ECL intensity vs time curves for the biosensor under continuous CV for six cycles. ECL curves were measured in 0.1 M PBS (pH 7.50, 0.10 M NaCl + 0.10 M NaH<sub>2</sub>PO<sub>4</sub>/Na<sub>2</sub>HPO<sub>4</sub>) containing 0.1 M TPrA. Scan rate: 100 mV·s<sup>-1</sup>, scan range: 0.2-1.25 V.

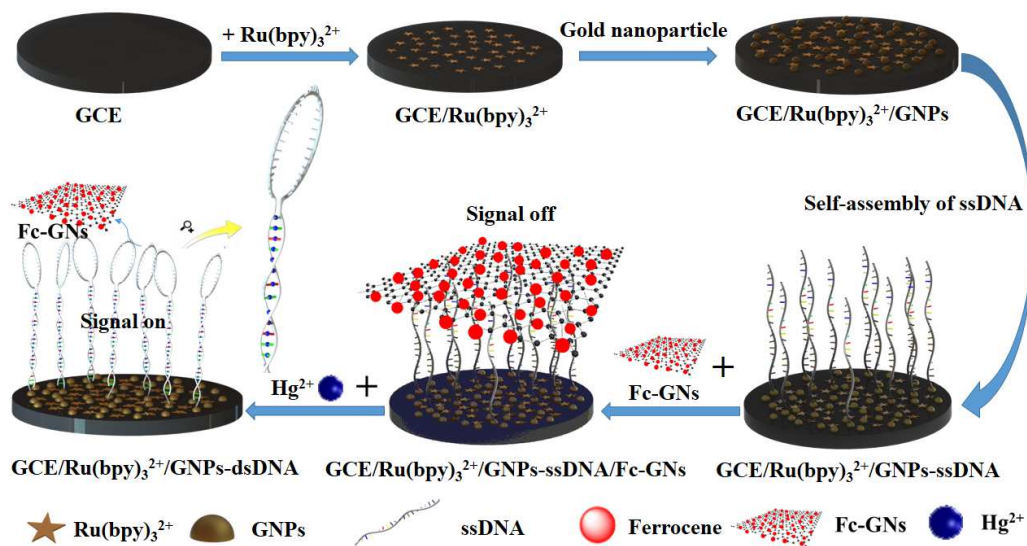
**Fig. 7** ECL intensity-time curves for the biosensor binding with various concentration of Hg<sup>2+</sup>. The concentrations of Hg<sup>2+</sup> were 0.05 nM (a), 0.1 nM (b), 1 nM (c), 10 nM (d), 20 nM (e), 50 nM (f) and 100 nM (g), respectively. Inset: The calibration curve of the ECL response as a function of the concentration of Hg<sup>2+</sup>. Error bars represent the standard deviation of five parallel experiments.

**Fig. 8** Effects of various metal ions and a mixture of metal ions (500 nM each for Cu<sup>2+</sup>, Zn<sup>2+</sup>, Ni<sup>2+</sup>, Cd<sup>2+</sup>, Mg<sup>2+</sup>, Fe<sup>2+</sup>, Ba<sup>2+</sup>, Pb<sup>2+</sup>, Cr<sup>3+</sup>, Co<sup>2+</sup>, Mn<sup>2+</sup>, Fe<sup>3+</sup>, Al<sup>3+</sup>, Ca<sup>2+</sup> and 10 nM

for  $\text{Hg}^{2+}$ ) on the ECL signal response measured by the optimal ECL biosensor. Error bars represent the standard deviation of three repetitive experiments.

**Table 1** Comparison of the sensitivity of different  $\text{Hg}^{2+}$  sensors

**Table 2** Determination the concentrations of  $\text{Hg}^{2+}$  in water samples using the proposed biosensing method and AFS<sup>a</sup> method.



Scheme 1

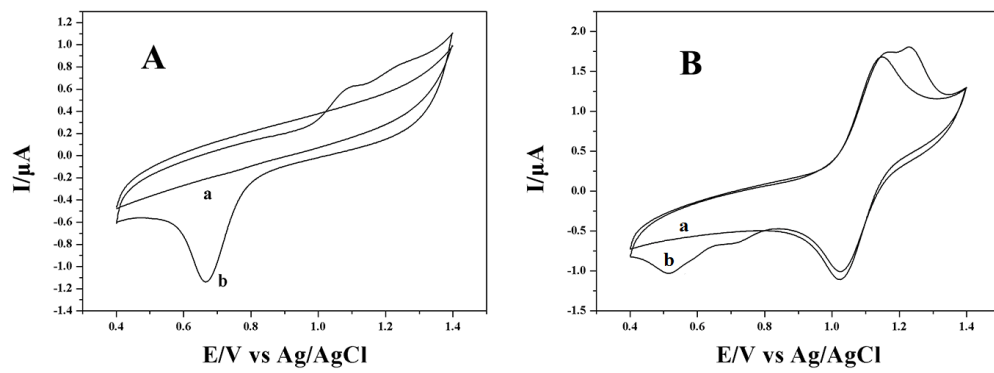


Fig. 1

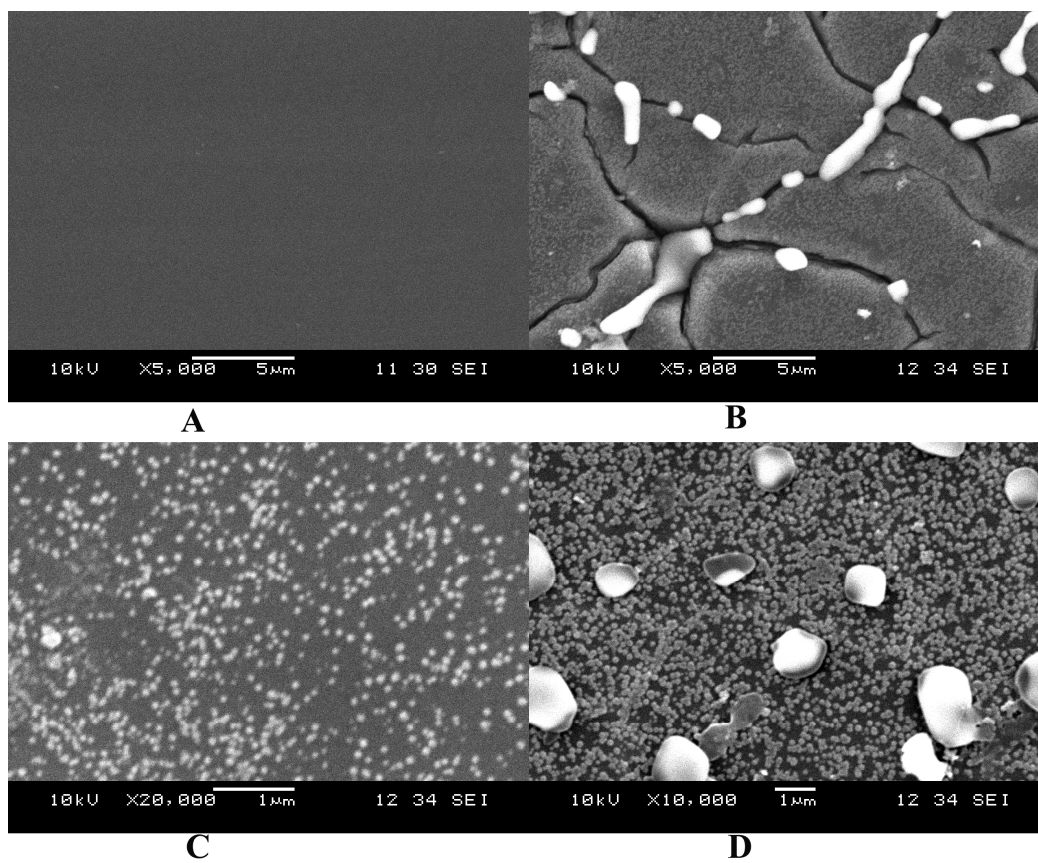


Fig. 2

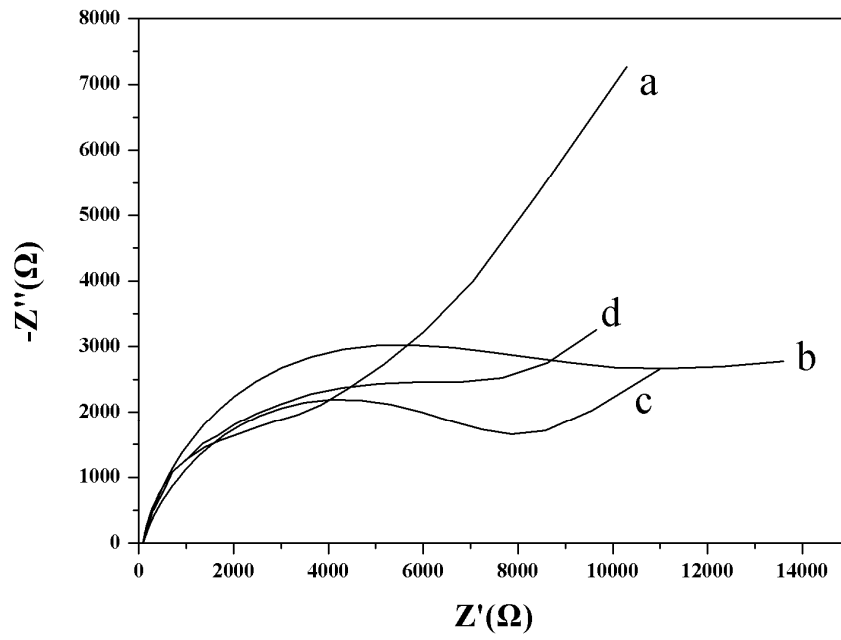


Fig. 3

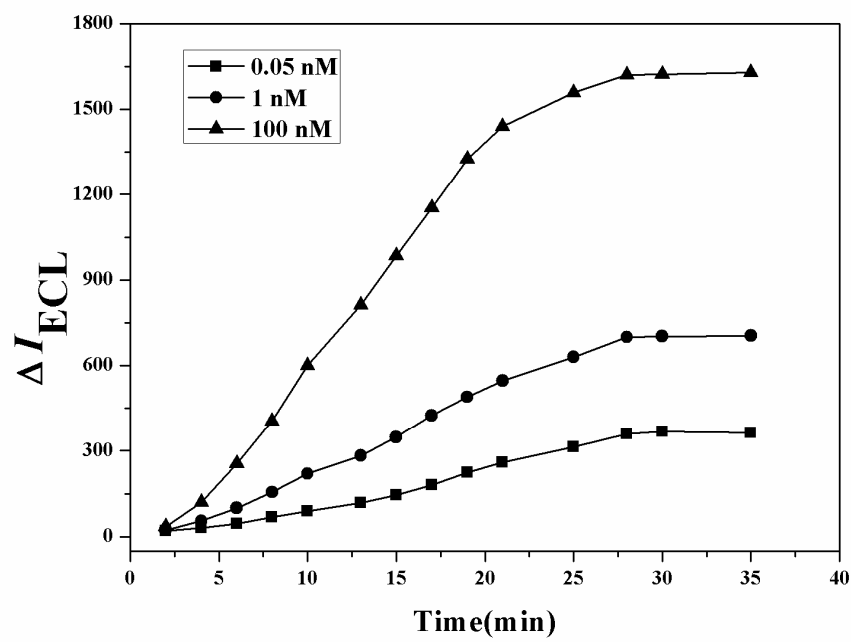


Fig. 4

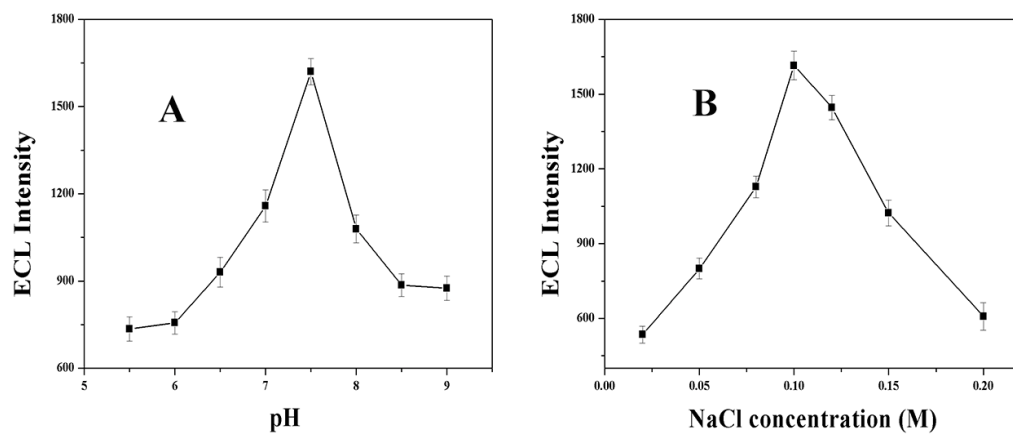


Fig. 5

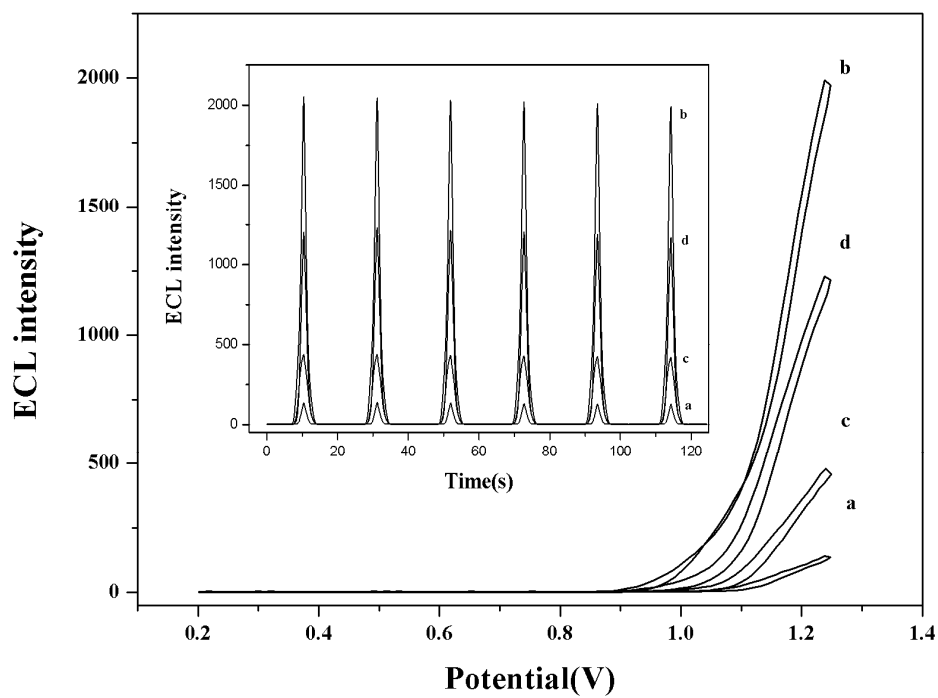


Fig. 6

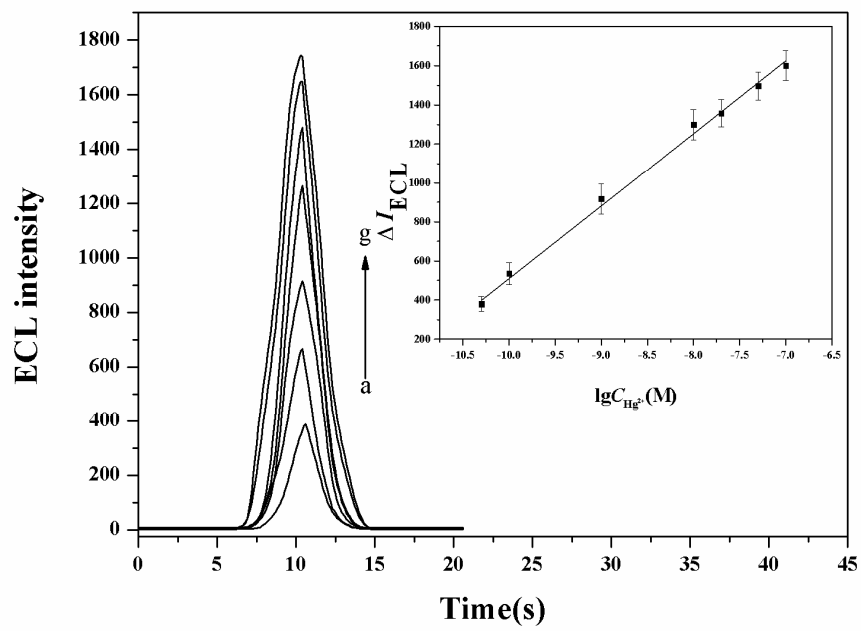


Fig. 7

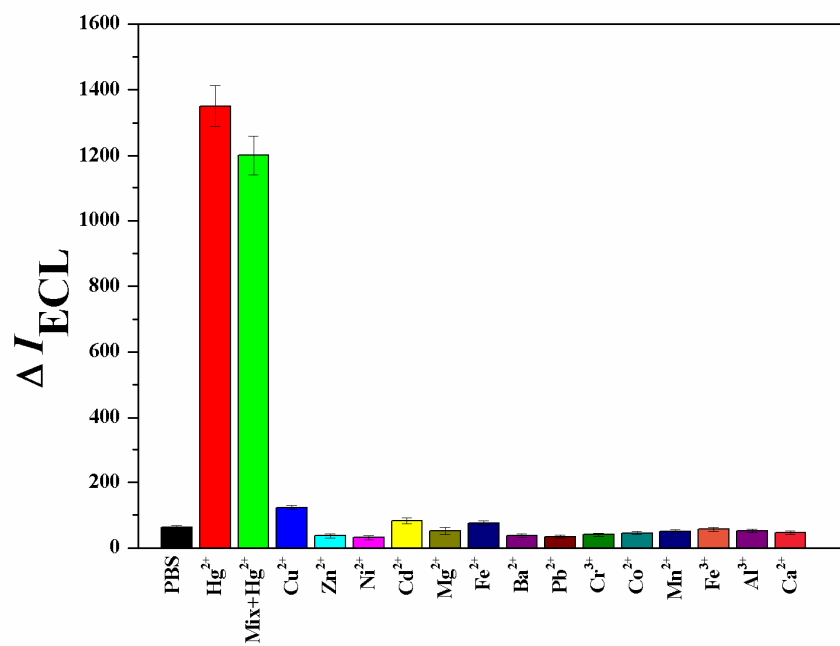


Fig. 8

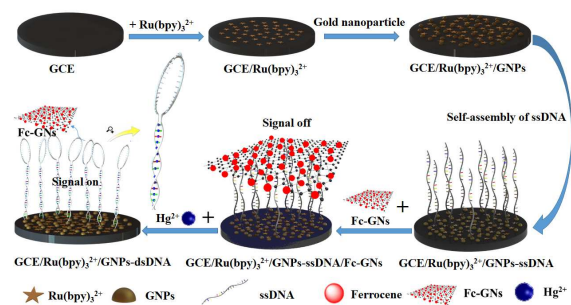
**Table 1** Comparison of the sensitivity of different Hg<sup>2+</sup> sensors

Detection method	Linear range	Limit of detection	Reference
Electrochemical method with nanoparticles-based signal amplification	Au 1 nM-0.1 μM	0.5 nM	31
Electrochemical sensor based on ferrocene-labeled DNA	0.1-2 μM	0.1 μM	32
Electrochemical sensor based on the cooperativity of proximate poly-T oligonucleotides	1 nM-2 μM	0.5 nM	33
Electrochemiluminescent biosensor using Ru(bpy) <sub>3</sub> <sup>2+</sup> -doped silica nanoparticles	5-500 nM	2.3 nM	34
Electrochemiluminescent method with Ru(phen) <sub>3</sub> <sup>2+</sup> as ECL probe	0.02-15 nM	20 pM	35
Electrochemiluminescent biosensor based on DNA-modified electrode and graphene via π-π interaction	0.05-100 nM	18 pM	This work

**Table 2** Determination the concentrations of  $\text{Hg}^{2+}$  in water samples using the proposed biosensing method and AFS<sup>a</sup> method.

Water sample	Biosensing method (nM)	AFS method (nM)	Relative deviation (%)
Xinhua River 1	$68.34 \pm 4.05$	$69.26 \pm 3.98$	-1.36
Xinhua River 2	$92.78 \pm 8.53$	$90.84 \pm 9.08$	2.37
Niutianyang bay 1	$106.86 \pm 7.89$	$110.12 \pm 5.68$	-3.84
Niutianyang bay 2	$143.67 \pm 9.64$	$141.79 \pm 7.31$	2.03

<sup>a</sup> All values were obtained as average of three repetitive determinations plus standard deviation.



An electrochemiluminescence biosensor with the quench pattern of ferrocene-graphene to  $\text{Ru}(\text{bpy})_3^{2+}$  via  $\pi$ - $\pi$  interaction between nucleotide and ferrocene-graphene and the detection limit of  $\text{Hg}^{2+}$  is 18 pM.